A 3D model of the peripheral benzodiazepine receptor and its implication in intra mitochondrial cholesterol transport

J.M. Bernassau,* J.L. Reversat,* P. Ferrara,† D. Caput,† and G. Lefur*

*Sanofi Recherche, Montpellier, France, †Sanofi Elf Bio-Recherches, Labege, France

A three-dimensional (3D) model of the peripheral benzodiazepine receptor (PBR) has been built using molecular dynamics simulations.

The transmembrane domain of the receptor has been modeled as five alpha-helices, which are not long enough to cross the entire bilayer membrane but correspond approximately to only one phospholipid layer. The receptor model has also been tested as a cholesterol carrier, and molecular dynamics simulations have shown that it could indeed accommodate a cholesterol molecule within the five helices. All three known PBR sequences have been modeled, and no significant difference has been found between them.

Keywords: molecular dynamics, benzodiazepine receptor, protein modeling

INTRODUCTION

Peripheral benzodiazepine receptors (PBR) have been described in various tissues such as kidney,[1] heart,[2] adrenals,[3] and even brain.[4] In contrast to classical central type benzodiazepine receptors, they are not coupled to the GABA gated chloride channels.[5] PBR are mainly located in the mitochondrial outer membrane,[6] and are involved in steroid synthesis.[7-13] In fact, PBRs mediate the delivery of cholesterol to the inner mitochondrial membrane where cholesterol oxidation begins.

The first step of steroid hormone synthesis[14] in steroidogenic cells is a C27 side chain cleavage producing pregnenolone. This reaction is catalyzed by a cytochrome P-450 scc located in the inner mitochondrial membrane. However, the rate-limiting step of the entire chain of catalytic events eventually leading to pregnenolone lies in the delivery of cholesterol to this P-450.[14,15]

The physiological significance of PBRs has in part been linked to this cholesterol delivery process.[11] The PBRs seem, however, to be involved in several other phenomena such as melanogenesis,[16] monocyte chemotaxis,[17] inhibition of cell proliferation,[18] and muscle contraction.[19]

PBRs can be identified by selective ligands such as [3H] Ro-54864 and [3H] PK-11195, or can be selectively labeled by photo affinity probes such as PK-14105.[20] Thanks to these ligands, the murine,[21] bovine,[22] and human[23] PBRs have been isolated, cloned, and sequenced. However, no detailed 3D crystal structure of PBRs is available and the aim of this paper is to build a 3D model of PBRs and to evaluate this model in the context of cholesterol transport.

METHODS

All calculations were performed with the SYBYL software[24] using the Amber united atom force field.[25,26]

The computer system was made of a network of SUNSPARC 2 workstations linked to a PS 390 (Evans and Sutherland) terminal for visualization.

The entire sequence of the human PBR was built using the SYBYL Biopolymer package and assigned an extended conformation. The five stretches corresponding to the five helices were then extracted, and their conformation set to that of an alpha helix. This allowed the amino acid residues within the transmembrane domain to be correctly numbered.

The helices could then be subjected to molecular dynamics simulations under constraints. Whenever necessary, the hydrogen bonds within the helices were replaced by C-N harmonic constraints (70 constraints, $r = 2.9$ Å, $k = 400$ kcal/mole/Å). This proved to be useful in the first steps of the modeling when the helices were brought together.

The dynamic runs were usually conducted by a progressive warming up of the system, e.g., 1 ps at 100 K and 200 K, followed by the dynamic simulation itself for 10 ps at 300 K and cooling at 100 K for 1 ps. Dynamic simulations were continued until no net energy evolution was noted for at least 10 ps. Energy minimization at the end of the dynamic simulations was performed by the Powell method with a termination criterion of gradient norm lower than 0.05.

To bring the five helices together in the first part of the simulation, 10 harmonic constraints were added from Gly19.CA to Asn92.CA, from Gly19.CA to Val115.C, from Ala50.C to Val115.C, from Ala50.C to Tyr152.N, and from Asn92.CA to Tyr152.N for the cytoplasmic side, and from Phe11.C to Tyr85.C, from Phe11.C to Thr123.C, from Ser58.C to Th123.C, from Ser58.C to Tyr140.O, and from Tyr85.C to Tyr140.O for the mitochondrial side of the transmembrane domain. These were defined as "range" constraints where the force constant was set to 50 kcal/mole/Å, the power to 2, and r_{min} and r_{max} were set 2 Å apart and progressively tightened from 20 Å to 10 Å. The energy in this process was lowered from 64 kcal/mole (five helices energy minimized, 20 Å apart) to -227 kcal/mole.

The human PBR was built as described above. The murine and bovine PBRs were built from the minimized structure of the human PBR, which was mutated in the desired positions. Molecular dynamics and energy minimization then yielded the refined receptors of roughly -200 kcal/mole internal energy (rat -230, bovine -238).

Accessible molecular surfaces were computed by the dot option of the Sybyl software using a density of 12 dots/Å^2.

The inter helix angles and distances were computed using programs developed for that purpose. The helix axes were determined by a least-squares-fit (IMSL program UMINF)[27] of the carbonyl carbons and amide nitrogens distances to a straight line. The other computations were straightforwardly implemented in AWK.[28]

The diameter of the inner channel delimited by the five helix bundle was determined by molecular dynamic simulations in which an atom of increasing diameter (vdW constant = .314) was pulled inside the protein (force constant = 0.5 Kcal/Å). The diameter was then taken as twice the vdW radius of the largest atom that could be carried across the protein.

The cholesterol molecule was first built and minimized using the Tripos all-atom force field. It was then stripped of its hydrogens, and its atoms were converted into Amber force field types for further calculations in relation to the PBR transmembrane domain.

To check whether the PBR could accommodate the cholesterol molecule, molecular dynamic simulations were performed using the five-helices PBR model previously obtained into which the cholesterol molecule was pulled by five new constraints linking Leu141.N, Gly10.N, Tyr127.N, Tyr62.N, and Leu84.N to the oxygen of the cholesterol molecule. When the cholesterol could no longer be pulled into the transmembrane domain it was pushed out by applying similar constraints linked to the molecule's C20 atom. The harmonic constraints for this simulation were set to *a very weak force constant* of 1 kcal/mole/Å. Some conformations of the complex were frozen at various stages of the translocation process, and the energy minimized. The energy difference between these conformations and a reference structure never exceeded 30 kcal/mole.

RESULTS

Before beginning the 3D modeling itself, the sequences of the three receptors[21-23] were aligned as shown in Figure 1. The extreme sequence conservation of some parts of the

receptors is readily apparent. The hydropathy[29] plot of the human sequence is presented in Figure 2. As previously pointed out,[21-23] five putative transmembrane helices can be distinguished. For the purpose of the present work, they

```
      10        20        30        40
MAPPWVPAVGFTLLPSLGGFLGAQYTRGEGFRWYASLQKPPWHPPR

MSQSWVPAVGLTLVPSLGGFMGAYFVRGEGLRWYASLQKPSWHPPR

MAPPWVPAMGFTLAPSLGCFVGSRFVHGEGLRWYAGLQKPSWHPPH
```

```
      50        60        70
WILAPIWGTLYSAMGYGSYMIWKELGGFSKEAV

WTLAPIWGTLYSAMGYGSYIIWKELGGFTEEAM

WVLGPVWGTLYSAMGYGSYLVWKELGGFTEKAV
```

```
80        90       100       110
VPLGLYAGQLALNWAWPPLFFGTRQMGWALVD

VPLGLYTGQLALNWAWPPIFFGARQMGWALVD

VPLGLYTGQLALNWAWPPIFFGARQMGWALVD
```

```
      120       130
LLLTGGMAAATAMAWHQVSPPAACLL

LMLVSGVATATTLAWHRVSPPAARLL

LLLVSGAAAATTVAWYQVSPLAARLL
```

```
140       150       160
YPYLAWLAFAGMLNYRMWQDNQVRRSGRRLSE

YPYLAWLAFATMLNYYVWRDNSGRRGGSRLTE

YPYLAWLAFATTLNYCVWRDNHGWHGGRRLPE
```

Figure 1. Alignment of the three receptor sequences. The beginning of each of the five helices has been aligned.
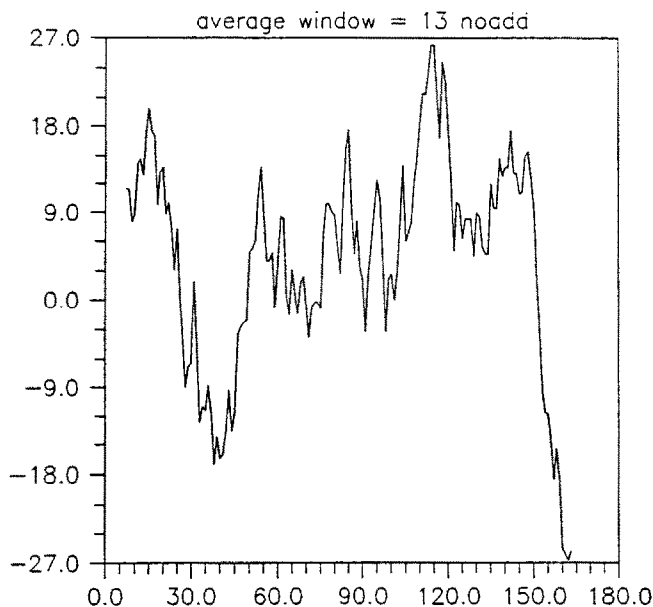
Figure 2. Hydropathy plot of human PBR. The averaging window width is thirteen amino acids. The hydropathy scale was taken from Doble et al.[20]

were assigned from Val 6 to Ala 23, from Trp 47 to Ser 64, from Val 80 to Pro 97, from Leu 112 to Trp 126 and from Tyr 138 to Trp 155. This yields the schematic structure of the receptor shown in Figure 3.

The presence of the transmembrane helices can further be corroborated by a comparison of their average hydrophobicity and helical hydrophobic moment[30] with that of other known transmembrane proteins. These values are presented for PBRs in Table 1 and fall within the range of the transmembrane helices. The values obtained for *bacteriorhodopsin* are also provided for comparison purposes. As evidenced in Table 1, the value pairs obtained for the helices of both proteins span similar ranges.

The presence of these putative amphipatic helices is even more markedly evidenced when they are built and colored, as in Color Plate 1, which clearly shows the presence of a hydrophilic side and a hydrophobic side.

The presence of several Proline residues in these sequences should be noted. Although considered a helix-breaking residue in globular proteins, proline is common in the sequence of transmembrane helices.[31,32]

The five helices were first built using standard amino acid geometries and were manually positioned so that their hydrophilic sides were facing the interior of the five-helix bundle. Although there are clearly many ways in which these helices may be placed with respect to one another, little attention was paid to the detailed arrangement of the side chains. The helices were simply disposed sequentially one after the other so that no side chain bumps would occur.

In the next step, the helices were constrained together as pictured on Color Plate 2 by a set of 2 × 5 harmonic constraints. Color Plate 2 shows how the constraints were set up in order to bring the five helices together. Initially, these were adjusted so that no force would be applied on the helices. Molecular dynamics simulations could then be started to heat up the system, followed by progressive tight-

ening of the constraints so that the helices would be brought together. A similar procedure has been described[33] for the simulation of ion channels.

This process could be continued with tighter and tighter constraints. Energy minimization after each dynamic run provided a measure of the internal energy of the system, which was shown to decrease as the helices were brought together, until they reached their minimum distance of approach. This decrease in energy can mainly be assigned to a decrease in the vdW and electrostatic energy contributions due to long-range interactions between the helices. If the constraints were further tightened, energy would increase

Table 1. Mean hydrophobicity and helical hydrophobic moment of the five putative helices of human PBR and bacteriorhodopsin

Residues[a]	$\langle H \rangle^b$	$\langle \mu H \rangle^c$	
6–23	0.21	0.12	
47–64	0.18	0.10	
80–97	0.14	0.09	PBR
112–126	0.19	0.02	
138–155	0.18	0.05	
Helix 1	0.21	0.11	
Helix 2	0.12	0.05	
Helix 3	0.05	0.12	
Helix 4	0.25	0.07	*Bacteriorhodopsin*
Helix 5	0.32	0.03	
Helix 6	0.11	0.14	
Helix 7	0.13	0.08	

[a] Taken from the human PBR sequence.
[b] Mean hydrophobicity.
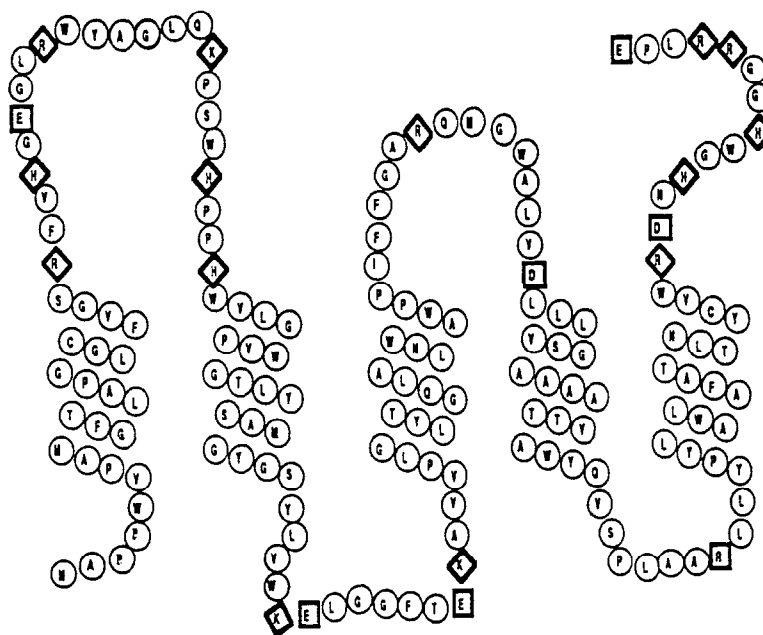[c] Mean helical hydrophobic moment.

Figure 3. Schematic of the folding proposed for the receptor.

sharply and distance constraints could no longer be satisfied. The system was left in a position where the helices were as close as possible, without a deteriorating rise in energy.

At this point, the constraints holding the helices together could be removed and the system could be shown to be stable under energy minimization and molecular dynamics at 300 K.

The resulting model is presented in Color Plate 3 together with *bacteriorhodopsin*. The packing of the two proteins can be seen to be similar. However, a more quantitative description of the models will help to clarify their similitudes and differences.

The five-helix bundle can be characterized by its geometry and its packing density.

The following procedure was used to obtain quantitative information about the inter helix contacts.[34] The helices were extracted one by one from the whole structure, and the accessible surface area of helix i was computed as $\{H_i\}$. Pairs of adjacent helices were then extracted, and for each member of the pair the accessible surface area of the helix i in contact with helix j was computed as $\{H_{i-j}\}$. The relative contact area of helix i in the i-j pair was then computed by $(\{H_i\} - \{H_{i-j}\})/\{H_i\}$. These values are given in Table 2 for the five-helix bundle and in Table 3 for *bacteriorhodopsin*. As can be seen from the comparison of the two tables, the relative losses in contact area for each of the two structures are very similar, indicating that the molecular dynamics resulted in a PBR model helix packing similar to that of *bacteriorhodopsin*.

Packing density is another characteristic parameter of protein structures. Table 4 shows the volume and density of the PBR model and *bacteriorhodopsin*. As can be seen, both structures reach very similar values of 5.89 ± 0.03 Å^3/atom, indicating again that the molecular dynamics yielded a structure of a density similar to another known transmembrane protein structure.

The geometry of the resulting model can also be characterized by the angles between the axes of the five helices. The mean axis of each helix was computed as the line minimizing the sum of the squares of the distances of the carbonyl carbons and amide nitrogens to that line.

Results are presented in Table 5 for the PBR model and for another crystallized five-helix bundle protein, the Apolp III.[35] As the latter protein is a much more elongated protein, the computation takes account of only a slice of the structure, the length of which is similar to that of the PBR model and is located on the N-terminal side. Shown in the table, the helices of the PBR model are more closely aligned than those the Apolipoprotein. Since we chose not to manually tilt the helical axes of our model, a rather good alignment could be expected to result from the procedure used. On the other hand, both the Apolipoprotein and *bacteriorhodopsin* adopt a packing profile in which the helices are somewhat tilted. However, the lack of helix tilting in the PBR model seemed preferable to an arbitrarily chosen tilt angle.

Another manner of evaluating helix packing is to consider the distances between the segments of the helix axes. These can be computed as follows. Along the axis of a helix obtained as previously described, the projections of the first and the last atom of the helix define a segment. One hundred evenly spaced points are selected on any two segments corresponding to two helices. For each point on a given

Table 2. Relative loss in accessible surface for each of the helices of the PBR model when it is brought into contact with its immediate neighbors. The element in row i and column j of the square matrix presented here is computed as $(\{H_i\} - \{H_{i-j}\})/\{H_i\}$

	1	2	3	4	5
1	.	17	.	.	17
2	22	.	26		.
3	.	26	.	26	.
4	.	.	22	.	26
5	14	.	.	19	.

Table 3. Relative loss in accessible surface for each of the helices of *bacteriorhodopsin* when it is brought into contact with its immediate neighbors. Values are computed as explained in Table 2.

	1	2	3	4	5	6	7
1	.	20	.	.	.	.	23
2	19	.	20	.	.	.	.
3	.	18	.	14	.	.	.
4	.	.	26	.	18	.	.
5	.	.	.	13	.	20	.
6	.	.	.	.	16	.	19
7	23	.	.	.	.	20	.

Table 4. The volume is given in Å^3 for all-atom structures. The average atomic volume V/N is therefore given in Å^3/atom. Only the transmembrane regions are considered in both structures

	PBR model	*Bacteriorhodopsin*
Volume	8045.3	16156.6
nb of atoms	1358	2764
V/N	5.92	5.86

Table 5. Angles between the axes of the helices in the PBR model (upper triangle) and in a part of the ApoLp III (lower triangle). Each axis is computed as the line minimizing the sum of the squares of the distances of the carbonyl carbons and amide nitrogens to that line

	1	2	3	4	5
1		6.3	9.9	8.4	16.9
2	18.4		3.6	4.6	11.8
3	8.7	15.8		6.0	10.3
4	9.3	21.4	5.6		8.6
5	17.5	5.1	12.9	18.4	

helix, the closest point of the other helix defines the minimum distance of the second helix to the point chosen on the first. Table 6 gives these minimum inter helix distances for the PBR model and for the previously described slice of the Apolp III protein. As can be seen from the table, the distances between adjacent helices are slightly larger for the lipoprotein than for the PBR model. Thus, the method used to generate the model results in a somewhat tighter packing than observed experimentally in a five-helix structure. It therefore seems that either the tilt or the longer length of the lipoprotein helices prevents them from reaching the tighter packing obtained by the molecular dynamic simulation.

Finally, the radius of the channel delineated by the five helices could be evaluated by pulling increasingly large atoms inside it. A molecular dynamics simulation was thus performed in which atoms of radius 2, 3, 4, and 6 Å were pulled inside the helical bundle. The results obtained clearly showed the pore radius to be less than 4 Å but larger than 3 Å. The atom of radius 3 Å could easily enter the channel without geometrical distortions or energy increase, whereas the atom of radius 4 Å could only be accommodated inside the helices by pushing them slightly away from their initial position. This process also resulted in an increased steric energy (ΔE = 15 kcal/mole).

In the next step, the previously obtained five-helix bundle was tested for cholesterol transport. The cholesterol molecule was built and parametrized in the Kollman united atom force field and positioned at the top of the five-helix channel.

It was clear that the cholesterol molecule could not enter the five-helix bundle without rearrangement of the side chains covering the inside of the channel. Molecular dynamics simulations were thus started, with the cholesterol molecule being pulled inside the helix bundle by five very weak harmonic constraints (Color Plate 4).

It was shown during these simulations that the internal energy of the system would not increase unduly, nor would the five helices be pushed further apart by the entering molecule. In fact, the cholesterol molecule could cross the five-helix bundle from one side to the other without serious geometrical modification or energy increase. Rather, the side chains of the amino acids covering the inner part of the receptor would simply move around so that they could accommodate the cholesterol molecule. Color Plate 5 shows this situation when the cholesterol is halfway through the receptor.

The simulation was terminated by "pushing" the choles-

terol out of the receptor by five harmonic constraints as above.

More insight into the details of the molecular dynamics simulation could be gained by analyzing the time course changes in some representative molecular features, which are displayed in Figure 4. As can be seen, the total energy (Figure 4a) decreases during the simulation. However, this energy includes the distance constraint term (Figure 4b). When the latter is subtracted (Figure 4c) the potential energy of the five-helix bundle–cholesterol complex is seen to be fluctuating without net energy drift.

Geometrical modifications can be seen to be minor when the root-mean-squared (rms) deviations of the helices are plotted against time as for helix 5 in Figure 4d. This however does not preclude side chain movements such as that of Tyr 62 which is seen in Figure 4e to rotate, being displaced when the cholesterol molecule travels by.

The same calculations were made in a similar fashion for the three known PBRs, namely human, murine, and bovine PBR. There were no significant energy differences in the results of these three calculations. However, no detailed analysis was performed in terms of side chain conformations within the various PBRs.

DISCUSSION

The peripheral benzodiazepine receptor has been shown to be involved in the transport of cholesterol from the outer to the inner mitochondrial membrane.[11] The present work was conducted to test this hypothesis at the molecular level, i.e., to check *whether a simple molecular model of the protein could be compatible with this transport,* and whether this molecular description could be used to make further hypotheses about the biological mechanism of the first step of stereoidogenesis in the mitochondria.

Although the *a priori* modeling of globular soluble proteins is still unrealistic at the present time, the field of transmembrane proteins has recently attracted considerable attention.[33,37–41] Primary focus has been on the receptors sharing some homology with *bacteriorhodopsin,*[36] whose structure has been described by electron diffraction studies. Thus, models of the alpha and beta adrenergic receptors,[42–44] dopamine D2 receptor,[45] and others, have been described. All these models have been based on the *bacteriorhodopsin* molecule.

The peripheral benzodiazepine receptor does not share homology with any other known protein, except a slight but significant relationship with the Crtk protein, one component of the seven-gene cluster of *Rhodobacter Capsulatus* responsible for carotenoid biosynthesis.[46,47] Unfortunately, the 3D molecular structure of Crtk is, like its function, unknown.

The molecular modeling of the peripheral benzodiazepine receptor has therefore to be started from basic principles. The five transmembrane helices could easily be located from hydropathy plots or visual inspection. It is noteworthy that in the sequences shown in Figure 1, the helix-connecting loops are alternately charged and neutral. This is in agreement with a transmembrane disposition of the mitochondrial receptor, the first heavily charged loop and the carboxy terminal end being located towards the cytoplasmic face of the membrane.

Table 6. Inter helix distances for the PBR model (upper) and a slice of the ApoLp III (lower). As the helix numbering of the latter protein differs from the PBR, neighboring helices are not necessarily contiguous numbers

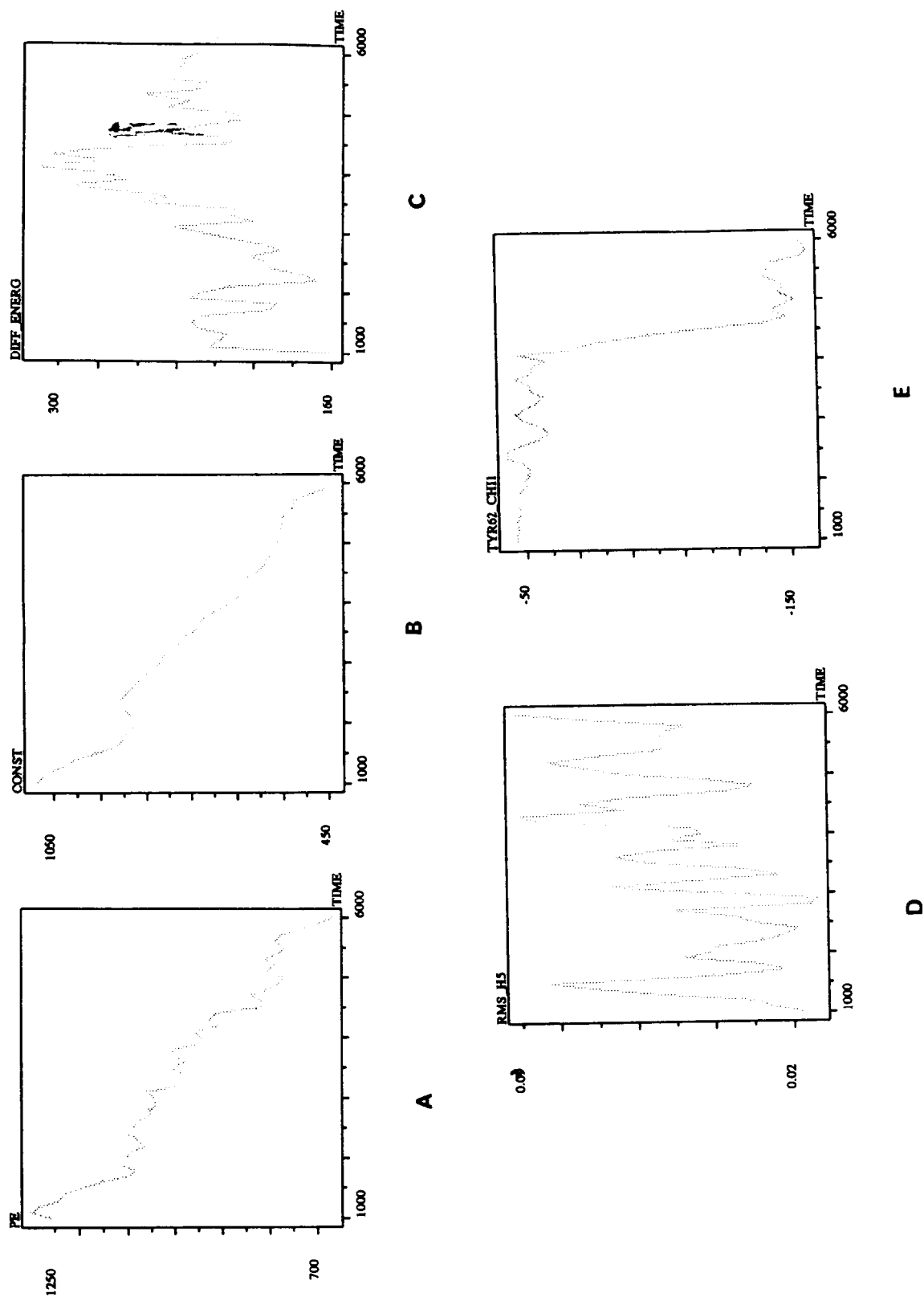|	1	2	3	4	5
1		7.4	12.4	12.7	8.8
2	13.9		8.2	14.6	13.0
3	17.1	8.3		8.6	12.3
4	9.4	11.0	8.9		8.1
5	8.6	9.6	12.6	11.8	

Figure 4. Plot of some representative molecular features during the molecular dynamic simulation.

Such five-helix membrane topology can also be found in the cyo C polypeptide, subunit 3 of the cytochrome o terminal oxidase complex,[48] the topology of which has been established by gene fusion.

The modeling was performed simply by forcing the five helices together so that they would be as close as possible to each other. Use was made of molecular dynamics simulations under constraints to position the amino acid side chains in their optimum configuration with respect to one another. The net result of this simulation is pictured in Color Plate 2.

The resulting structure was found to possess geometrical features similar to those of bacteriorhodopsin (accessible surface, packing density). However, comparison with an unrelated five-helix protein (Apolp III) showed that the modeling procedure resulted in a structure in which the helices had a smaller tilt angle and were relatively more densely packed. The inner radius of the modeled five-helix bundle, which was evaluated to lie between 3 Å and 4 Å, could therefore be underestimated.

This modeling process could not be extended to the helix-connecting loops. Although the shortest of them could have been tentatively positioned, it was felt that the first and second loops, as well as the carboxy terminal sequences, were of a length that would preclude any significant modeling. Therefore, only the five transmembrane helices are taken into consideration in the present study. In particular, this prevented us from studying any ligand-binding process that involved these cytosolic charged loops.

However, the previously described five-helix model could be tested as a cholesterol carrier. We chose to test the hypothesis of a cholesterol molecule entering the channel formed by the helices. Since the receptor presents a hydrophilic, but uncharged, molecular surface on its inner face, it was felt that the amphiphilic cholesterol molecule could be accommodated within this channel.

Here again, use was made of molecular dynamics simulations under constraints, and it was shown that the cholesterol could indeed be translocated from one side of the five-helix bundle to the opposite side, without geometric distortions of helix packing or significant internal energy increase. This translocation was obtained by rotation of the amino acid side chains lying inside the five-helix channel in a way somewhat resembling the bristles of a brush. This side chain movement is necessary for the cholesterol to be accommodated within the helix channel. Otherwise, and in the absence of cholesterol, the inner channel looks closed, being occupied by the amino acid side chains.

The peripheral benzodiazepine receptor was thus shown to be able to accommodate a cholesterol molecule within the channel formed by the five transmembrane helices (Color Plate 5). This simulation must be qualitatively interpreted in terms of steric interactions. In particular, no quantitative energy considerations were attempted.

However, comparison with bacteriorhodopsin as well as simple geometric measurements proved that the length of the helices did not allow them to cross the entire mitochondrial membrane. In fact, the length of a receptor helix seems to be close to half the length of a bacteriorhodopsin helix (Color Plate 6) implying that the benzodiazepine receptor would be anchored in the outer layer of the outer bilayer membrane of the mitochondrion.

This half membrane positioning can be interpreted in

relation to the function of the peripheral benzodiazepine receptor as a cholesterol transporter. Since cholesterol is soluble in the lipid layers, it can be imagined that the receptor's function is to carry the cholesterol molecules from the outer lipid monolayer of the outer mitochondrial membrane to the inner lipid monolayer of that same membrane (Figure 5). The corresponding flip-flop movement of molecules from one side of a bilayer membrane to the other is known to be a rare molecular event and could thus be actively catalyzed.

The receptor could act as a "shield" in this function, hiding the cholesterol from the hydrophobic membrane inner medium. The molecular details of this phenomenon as well as its energetics cannot be simulated properly at the present time.

It is particularly noteworthy, although not very surprising in view of the very strong sequence homology of the three known PBRs, that the overall conclusions drawn from the previous study of human PBR are similar for the three PBRs. This, of course, supports the view that this receptor has the same physiological role in all the species studied so far.

The hypothesis of half membrane positioning of the PBRs is supported by the fact that endogenous ligands of the receptor bear the same alpha-helix structure. DBI is a 9 kDa neuropeptide[49] which is processed into several shorter peptides, among which ODN is selective for the central benzodiazepine receptor and TTN is selective for the peripheral receptor, the subject of this study.

It is particularly noteworthy that TTN, but not ODN, possesses an amphiphilic alpha-helix of the same length as the helices of the PBRs.[50]

In conclusion, the molecular model of the peripheral benzodiazepine receptor presented in this paper proposes a new mechanistic hypothesis for the physiological role of this protein in the steroidogenic pathway.
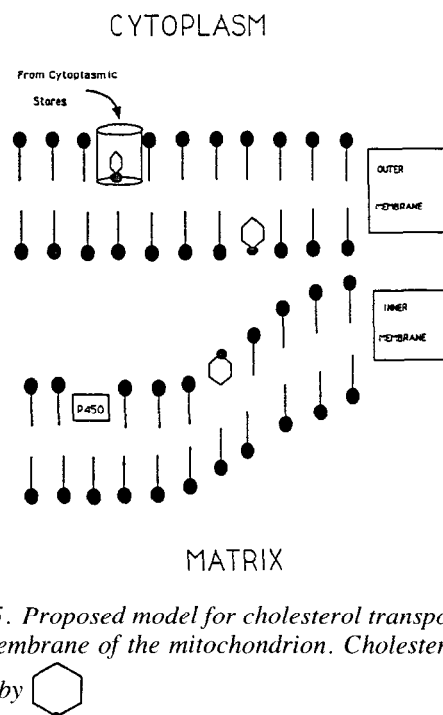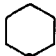

Figure 5. Proposed model for cholesterol transport into the inner membrane of the mitochondrion. Cholesterol is symbolized by ⬡

The transportation model described here is fully compatible with previous views on the subject but adds interesting molecular aspects on the detailed manner by which cholesterol could reach the inner mitochondrial membrane.

The three PBR sequences studied show neither significant geometric nor energetic differences, a fact compatible with a common transportation model in all species.

As previously stated, the modeling cannot at the present time take into consideration the inter helix loops as well as the N and C terminal chains. No hypothesis can therefore be made on the binding of agonist or antagonist molecules to the receptor.

The hypothesis proposed in the present paper is not easily tested because of the difficulty in setting up functional tests on intracytoplasmic organelles. Moreover, such a test would need to discriminate between the two mitochondrial membranes.

It is hoped, however, that it will be possible to test the topological hypothesis underlying the helix bundle by poly or monoclonal antibodies or by gene fusion proteins. Furthermore, mutagenesis experiments aimed at defining the importance of the various parts of the structure and detailing the binding contributions of specific amino acids are under way and should help to create a full molecular picture of the peripheral benzodiazepine receptor.

ACKNOWLEDGMENTS

REFERENCES

1 Taniguchi, T., Wang, J.K.T., and Spector, S. [3H] diazepam binding sites on rat heart and kidney. Biochem. Pharmacol. 1982, 31, 589–590

2 Le Fur, G., Vaucher, N., Perrier, M.L., Flamier, A., Benavides, J., Renault, C., Dubroeucq, M.C., Gueremy, C., and Uzan, A. Differentiation between two ligands for peripheral benzodiazepine binding sites, [3H] RO5–4864 and [3H] PK 11195, by thermodynamic studies. Life Sci. 1983, 33, 449–457

3 Benavides, J., Malgouris, C., Imbault, F., Begassat, F., Uzan, A., Renault, C., Dubroeucq, M.C., Gueremy, C., and Le Fur, G. "Peripheral-type" benzodiazepine binding sites in rat adrenals: Binding studies with [3H] PK 11195 and autoradiographic localization. Arch. Int. Pharmacodyn. 1983, 226, 38–49

4 Benavides, J., Quarteronet, D., Imbault, F., Malgouris, C., Uzan, A., Renault, C., Dubroeucq, M.C., Gueremy, C., and Le Fur, G. Labeling of "peripheral-type" benzodiazepine bindings sites in the rat brain by using [3H] PK 11195, an isoquinoline carboxamide derivative: Kinetic studies and autoradiographic localization. J. Neurochem.1983, 41, 1744–1750

5 Costa, E. and Guidotti, A. Molecular mechanisms in the receptor action of benzodiazepines. Ann. Rev. Pharmacol. Toxicol. 1979, 19, 531–545

6 Anholt, R.R.H., Pedersen, P.L., De Souza, E.B., and Snyder, S.H. The peripheral-type benzodiazepine receptor localization to the outer membrane. J. Biol. Chem. 1986, 261, 576–583

7 Anholt, R.R.H., De Souza, E.B., Kuhar, M.J., and Snyder, S.H. Depletion of peripheral-type benzodiazepine receptors after hypophysectomy in rat adrenal gland and testis. Eur. J. Pharmacol. 1985, 110, 41–46

8 Besman, M.J., Yanagibashi, K., Lee, T.D., Kawamura, M., Hall, P.F., and Shively, J.E. Identification of des-(Gly-Ile)-endozepine as an effector of corticotropin dependent adrenal steroidogenesis: Stimulation of cholesterol delivery is mediated by the peripheral benzodiazepine receptor. Proc. Natl. Acad. Sci. USA. 1989, 86, 4897–4901

9 Mukhin, A.G., Papadopoulos, V., Costa, E., and Krueger, K.E. Mitochondrial benzodiazepine receptors regulate steroid biosynthesis. Proc. Natl. Acad. Sci. USA. 1989, 86, 9813–9816

10 Papadopoulos, V., Mukhin, A.G., Costa, E., and Krueger, K.E. The peripheral-type benzodiazepine receptor is functionally linked to Leydig cell steroidogenesis. Proc. Natl. Acad. USA. J. Biol. Chem. 1990, 265, 3772–3779

11 Krueger, K.E. and Papadopoulos, V. Peripheral-type benzodiazepine receptors mediate translocation of cholesterol from outer to inner mitochondrial membranes in adrenocortical cells. J. Biol. Chem. 1990, 265, 15015–15022

12 Papadopoulos, V., Nowzari, F.B., and Krueger, K.E. Hormone stimulated steroidogenesis is coupled to mitochondrial benzodiazepine receptors. J. Biol. Chem. 1991, 266, 3682–3687

13 Krueger, K.E. and Papadopoulos, V. Mitochondrial benzodiazepine receptors and the regulation of steroid biosynthesis. Ann. Rev. Pharmacology Toxicology. 1992, 32, 211–237

14 Hall, P.F. Cellular organization for steroidogenesis. Int. Rev. Cytology. 1984, 86, 53–95

15 Yanagibashi, K., Ohno, Y., Kazwamura, M., and Hall, P.F. The regulation of intracellular transport of cholesterol in Bovine Adrenal Cells: Purification of a novel protein. Endocrinology. 1988, 23, 2075–2082

16 Matthew, E., Laskin, J.D., Zimmerman, E.A., Weinstein, I.B., Hsu, K.C., and Engelhardt, D.L. Benzodiazepines have high affinity binding sites and induce melanogenesis in B16/C3 melanoma cells. Proc. Natl. Acad. Sci. USA. 1981, 78, 3935–3939

17 Ruff, M.R., Pert, C.B., Weber, R.J., Wahl, L.M., Wahl, S.M., and Paul, S.M. Benzodiazepine receptor mediated chemotaxis of human monocytes. Science. 1985, 229, 1281–1283

18 Wang, J.K.T., Morgan, J.I., and Spector, S. Differentiation of Friend erythroleukemia cells induced by benzodiazepines. Proc. Natl. Acad. Sci. USA. 1984, 81, 3770–3772

19 Benavides, J., Guilloux, F., Allam, D.E., Uzan, A., Mizoule, J., Renault, C., Dubroeucq, M.C., Gueremy, C., and Le Fur, G. Opposite effects of an agonist, RO 5-4864, and an antagonist PK 11195 of the peripheral benzodiazepine binding sites on audiogenic seizures in DBA/2 J mice. Life Sci. 1984, 34, 2613–2620

20 Doble, A., Ferris, O., Burgevin, M.C., Menager, J., Uzan, A., Dubroeucq, M.C., Renault, C., Gueremy,

C., and Le Fur, G. Photoaffinity labeling of peripheral-type benzodiazepine binding sites. *Mol. Pharmacol.* 1986, **31**, 42–49

21 Sprengel, R., Werner, P., Seeburg, P.H., Mukhin, A.G., Rita Santi, M., Grayson, D.R., Guidotti, A., and Krueger, K.E. Molecular cloning and expression of cDNA encoding a peripheral-type benzodiazepine receptor. *J. Biol. Chem.* 1989, **264**, 20415–20421

22 Parola, A.L., Stump, D.G., Pepperl, D.J., Krueger, K.E., Regan, J.W., and Laird, H.E. Cloning and expression of a pharmacologically active unique bovine peripheral-type benzodiazepine receptor isoquinoline binding protein. *J. Biol. Chem.* 1991, **266**, 14082–14087

23 Riond, J., Mattei, M.G., Kaghad, M., Dumont, X., Guillemot, J.C., Le Fur, G., Caput, D., and Ferrara, P. Molecular cloning and chromosomal localization of a human peripheral-type benzodiazepine receptor. *Eur. J. Biochem.* 1991, **195**, 305–311

24 SYBYL, a molecular modeling package. Tripos Associates, Inc. 1699 S. Hanley Rd., Suite 303, St Louis, MO 63144, USA

25 Weiner, S.J., Kollman, P.A., Nguyen, D.T., and Case, D.A. An all-atom force field for simulations of proteins and nucleic acids. *J. Comput. Chem.* 1986, **7**, 230–252

26 Weiner, S.J., Kollman, P.A., Case, D.A., Chandra Singh, U., Ghio, C., Alagona, G., Profeta, S., and Weiner, P. A new force field for molecular mechanical simulation of nucleic acids and proteins. *J. Amer. Chem. Soc.* 1984, **106**, 765–784

27 IMSL. Version 2.0, 2500 City West Bld, Houston, TX, USA

28 Aho, A.V., Kernigan, B.W., and Weinberger, P.J. The AWK language. AT&T. 1988

29 Kyte, J. and Doolittle, R.F. A simple method for displaying the hydropathic character of a protein. *J. Mol. Biol.* 1982, **157**, 105–132

30 Eisenberg, D., Weiss, R.M., and Terwilliger, T.C. The helical hydrophobic moment: A measure of the amhiphilicity of a helix. *Nature.* 1982, **299**, 371

31 Deber, C.M., Glibowicka, M., and Wooley, G.A. Conformation of proline residues in membrane environment. *Biopolymers.* 1990, **29**, 149–157

32 Sankararamakrishnan, R. and Vishveshwara, S. Conformational studies on peptides with proline in the right-handed alpha-helical region. *Biopolymers.* 1990, **30**, 287–298

33 Pullman, A. Contribution of theoretical chemistry to the study of ion transport through membranes. *Chem. Rev.* 1991, **91**, 793–812

34 Richmond, T.J. and Richards, F.M. Packing of α-helices geometrical constraints and contact areas. *J. Mol. Biol.* 1978, **199**, 537–555

35 Breiter, D.R., Kanost, M.R., Benning, M.M., Wesenberg, G., Law, J.H., Wells, M.A., Rayment, I., and Holden, H.M. Molecular structure of an Apolipoprotein determined at 2.5-Å resolution. *Biochemistry.* 1991, **30**, 603–608

36 Henderson, R., Baldwin, J.M., Ceska, T.A., Zemlin,

F., Beckmann, E., and Downing, K.H. Model for the structure of bacteriorhodopsin based on high-resolution electron cryo-microscopy. *J. Mol. Biol.* 1990, **213**, 899–929

37 Findlay, J. and Eliopoulos, E. Three-dimensional modeling of G protein linked receptors. *Trends Pharmacol. Sci.* 1990, **11**, 492–499

38 Jähnig, F. Structure predictions of membrane proteins are not that bad. *Trends Biochem. Sci.* 1990, **15**, 93–95

39 Fasman, G.D. and Gilbert, W.A. The prediction of *trans* membrane protein sequence and their conformation: An evaluation. *Trends Biochem. Sci.* 1990, **15**, 89–92

40 Crimi, M. and Esposti, M.D. Structural predictions for membrane proteins: The dilemma of hydrophobicity scales. *Trends Biochem. Sci.* 1991, **16**, 119

41 Dohlman, H.G., Thorner, J., Caron, M.G., and Lefkowitz, R.G. Model systems for the study of seven transmembrane segment receptors. *Ann. Rev. Biochem.* 1991, **60**, 653–688

42 Strader, C.D., Sigal, I.S., and Dixon, R.A.F. Structural basis of beta adrenergic receptor function. *FASEB J.* 1989, **3**, 1825–1832

43 Venter, J.C., Fraser, C.M., Kerlavage, A.R., and Buck, M.A. Molecular biology of adrenergic and muscarinic cholinergic receptors. *Biochem. Pharmacol.* 1989, **38**, 1197–1208

44 Emorine, L.J., Feve, B., Pairault, J., Briend-Sutren, M.M., Marullo, S., Delavier-Klutchko, C., and Strosberg, D.A. Structural basis for functional diversity of beta-1, beta-2 and beta-3 adrenergic receptors. *Biochem. Pharmacol.* 1991, **41**, 853–859

45 Dahl, S.G., Edvardsen, O., and Sylte, I. Molecular dynamics of dopamine at the D2 receptor. *Proc. Natl. Acad. Sci. USA.* 1991, **88**, 8111–8115

46 Armstrong, G.A., Alberti, M., Leach, F., and Hearst, J.E. Nucleotide sequence, organization, and nature of the protein products of the carotenoid biosynthesis gene cluster of *Rhodobacter Capsulatus. Mol. Gen. Genet.* 1989, **216**, 254–268

47 Baker, M.E. and Fanestil, D.D. Mammalian peripheral-type benzodiazepine receptor is homologous to CrtK protein of *Rhodobacter Capsulatus* a photosynthetic bacterium. *Cell.* 1991, **65**, 721–722

48 Chepuri, V. and Hennis, R.B. The use of gene fusions to determine the topology of all the subunits of the cytochrome o terminal oxydase complex of *E. Coli. J. Biol. Chem.* 1990, **265**, 12978–12986

49 Costa, E. and Guidotti, A. Diazepam binding inhibitor (DBI): A peptide with multiple biological actions. *Life Sci.* 1991, **49**, 325–344

50 Berkovich, A., Mc Phie, P., Campagnone, M., Guidotti, A., and Hensley, P. A natural processing product of rat diazepam binding inhibitor triakon-tetraneuropeptide (Diazepam binding inhibitor 17–50) contains an alpha-helix, which allows discrimination between benzodiazepine binding site subtypes. *Molec. Pharmacol.* 1989, **37**, 164–172